

# Novel Thermally Stable Triarylamine-Containing Aromatic Polyamides Bearing Anthrylamine Chromophores for Highly Efficient Green-Light-Emitting Materials

HUNG-JU YEN, GUEY-SHENG LIOU

Functional Polymeric Materials Laboratory, Institute of Polymer Science and Engineering,  
National Taiwan University, Taipei 10617, Taiwan, Republic of China

Received 23 June 2008; accepted 21 August 2008

DOI: 10.1002/pola.23040

Published online in Wiley InterScience (www.interscience.wiley.com).

**ABSTRACT:** A series of novel polyamides with pendent anthrylamine units were prepared via the direct phosphorylation polycondensation from various diamines and the anthrylamine-based aromatic dicarboxylic acid, 9-[*N,N*-di(4-carboxyphenyl)amino]anthracene (4). The aromatic polyamides had useful levels of thermal stability associated with relatively high softening temperatures ( $T_g$ ) (290–300 °C), 10% weight-loss temperatures ( $T_d^{10}$ ) nearly in excess of 550 °C, and char yields at 800 °C in nitrogen higher than 60%. These aromatic polyamides **I** exhibited highly photoluminescence quantum yield in NMP solution ranges from 55% for **Ia** to 74% for **Ie** due to the introduction of anthrylamine chromophores. Cyclic voltammograms of the polyamide films cast onto an indium-tin oxide (ITO)-coated glass substrate exhibited one oxidation and reduction couples ( $E_{onset}$ ) around 1.10 and –1.50 V versus Ag/AgCl in acetonitrile (CH<sub>3</sub>CN) and DMF solutions, respectively. © 2008 Wiley Periodicals, Inc. *J Polym Sci Part A: Polym Chem* 46: 7354–7368, 2008

**Keywords:** fluorescence; high performance polymers; polyamides

## INTRODUCTION

Polymeric light-emitting diodes (PLEDs) have been widely studied, and the most efficient devices with a layered architecture reported are multilayer devices which comprise a sequence of a hole-transporting layer, an emitting layer, and an electron-transporting layer.<sup>1</sup> However, the assembly of multilayer devices requires careful selection of solvents to avoid compromise of previously deposited films. To solve this problem, blended materials that contain mixtures of hole transporters, electron transporters, and emitters can be used to form efficient single-layer devices.<sup>2</sup> The advantage of the latter approach is that phase

separation of the different components can be achieved providing the necessary exciton confinement. However, metastable phase separation may also reduce lifetimes for these devices. Alternatively, it is possible to covalently incorporate the electron-transport units in the polymer main chain to improve device performance.

Many emitting materials have been designed and used in LEDs; however, high-performance light emitting ones are rare because of the intrinsic wide band-gap required for such materials. Many hole transporting materials have been tried for light emission.<sup>3</sup> Anthracene itself is known as a hole- and electron-transporting blue light emitter.<sup>4</sup> Their derivatives have interesting photoluminescence (PL) and electrochemical properties,<sup>5</sup> and form an important class of highly efficient stable blue-light emitting materials.<sup>6</sup> It has been suggested that nonplanar derivatives of anthracene

Correspondence to: G.-S. Liou (E-mail: gsliau@ntu.edu.tw)

*Journal of Polymer Science: Part A: Polymer Chemistry*, Vol. 46, 7354–7368 (2008)  
© 2008 Wiley Periodicals, Inc.

by steric factors may hinder close packing and improve the device performance; hence the anthracene derivatives have been extensively studied in applications such as LEDs.<sup>7</sup>

An emitter with either a hole- or electron-transporting capability is beneficial, thus can simplify the device structure. Most of the hole-transporting materials which contain amine functionalities lack sufficient emission characteristics due to reductive quenching.<sup>8</sup> On the other hand, strong or bright luminescent materials may be obtained by incorporating chromophore units to the amine derivatives. Research by our laboratory<sup>9</sup> and others<sup>10</sup> aimed at the development of triaryl amines incorporated with photoluminescent chromophores has resulted in a new class of compounds capable of emitting blue or green colors. Triaryl amines capable of emitting blue light appear to be interesting because they can not only be used as a blue-light source, but also as host for downhill energy transfer to green- or red-emitting materials. Triaryl amines also have attracted considerable interest as hole transport materials for use in multilayer organic electroluminescence (EL) devices due to their relatively high mobility and their low ionization potentials.<sup>11</sup> The feasibility of utilizing spin-coating and inkjet printing processes for large-area EL devices and the possibilities for various chemical modifications (to improve emission efficiencies and allow patterning) make polymeric materials containing triarylamine units very attractive.<sup>12</sup>

Wholly aromatic polyamides are characterized as highly thermally stable polymers with a favorable balance of physical and chemical properties. However, the rigidity of the backbone and strong hydrogen bonding result in high melting temperatures or glass-transition temperatures and limited solubility in most organic solvents.<sup>13</sup> These properties make them generally intractable or difficult to process, thus restricting their applications in some fields. To overcome these limitations, polymer-structure modification becomes necessary. One of the common approaches for increasing the solubility and processability of aromatic polymers without sacrificing high thermal stability is the introduction of bulky, packing-disruptive groups into the polymer backbone.<sup>14</sup> Recently, we have reported the synthesis of soluble aromatic poly(amine-amide)s bearing naphthylamine<sup>9(d)</sup> and carbazole<sup>9(b)</sup> chromophores in the main chain with high quantum yield of 15 and 46% in *N*-methyl-2-pyrrolidone (NMP), respectively. Because of the introduction of bulky, propeller-shaped triphenyl-

amine units along the polymer backbone, all the polymers were amorphous with good solubility in many aprotic solvents and film-forming capability, and exhibited high thermal stability.<sup>15</sup>

In this contribution, we describe the synthesis of novel anthrylamine-based diacid monomer, 9-[*N,N*-di(4-carboxyphenyl)amino]anthracene (**4**), and the corresponding aromatic polyamides. The incorporation of bulky, hindered rotation, and kinked 9-anthryldiphenylamine moieties into polymer backbone could enhance the solubility by reducing interchain interactions and stacking efficiency with retention of excellent thermal stability. The general properties such as solubility and thermal properties are described. Furthermore, the photophysical, electrochemical, and photoluminescent properties of these polyamides were also investigated and are compared with those of structurally related ones from 1-[*N,N*-di(4-carboxyphenyl)amino]naphthalene and 4,4'-dicarboxytriphenylamine.

## EXPERIMENTAL

### Materials

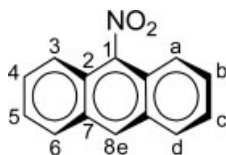
1-[*N,N*-di(4-carboxyphenyl)amino]naphthalene<sup>9(a)</sup> (mp: 316–318 °C) and 4,4'-dicarboxytriphenylamine<sup>16</sup> (mp: 313–315 °C) were synthesized by the cesium fluoride-mediated condensation of 1-naphthylamine and aniline with 4-fluorobenzonitrile, followed by the alkaline hydrolysis of the intermediate dinitrile compound according to a previously reported procedure, respectively. Commercially available aromatic diamines such as *p*-phenylenediamine (**5a**) (TCI) was purified by sublimation *in vacuo*, 4,4'-oxydianiline (**5b**) and 9,9-bis(4-aminophenyl)fluorene (**5c**) (TCI) were purified by recrystallization in ethanol 2,2'-bis(4-aminophenoxy)-1,1'-binaphthyl (**5d**) and 2,2'-bis(4-amino-2-trifluoromethylphenoxy)biphenyl (**5e**) were synthesized previously in our laboratory.<sup>17</sup> Anhydrous calcium chloride (CaCl<sub>2</sub>) was dried under vacuum at 180 °C for 8 h. Tetrabutylammonium perchlorate (TBAP) (Acros) was recrystallized twice by ethyl acetate under nitrogen atmosphere and then dried *in vacuo* prior to use. All other reagents were used as received from commercial sources.

### Monomer Synthesis

#### 9-Nitroanthracene (**1**)

In a 500-mL three-neck round-bottomed flask equipped with a stirring bar under nitrogen

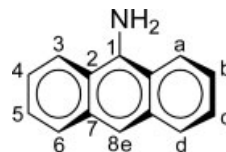
atmosphere, 9.14 g (50.23 mmole) of anthracene was suspended in 80 mL of glacial acetic acid at 20–25 °C, and 3.49 g (55.40 mol) of concentrated nitric acid (100%) was added slowly from dropping funnel for 1 h. Then, the reaction was continued for 3 h. A mixture of 25 mL (300 mmole) of concentrated hydrochloric acid (37 wt %) and 25 mL of glacial acetic acid was added slowly to the reaction solution with stirring to obtain pale-yellow precipitate of 9-nitro-10-chloro-9,10-dihydroanthracene which was washed by water until neutral. The product was triturated thoroughly with 60 mL of warm (60–70 °C) 10% sodium hydroxide solution. The crude orange nitroanthracene was treated with four 40 mL portions of 10% sodium hydroxide solution then washed thoroughly with warm water until neutral to litmus. The crude 9-nitroanthracene was recrystallized from methanol to afford 10.80 g (96% in yield) of yellow needles with mp of 150–151 °C (measured by DSC at 10 °C/min) (lit.<sup>18</sup> 145 °C). FTIR (KBr): 1518 cm<sup>-1</sup> (NO<sub>2</sub> stretch). <sup>1</sup>H NMR (DMSO-*d*<sub>6</sub>, δ, ppm): 7.62 (t, 2H, H<sub>c</sub>), 7.73 (t, 2H, H<sub>b</sub>), 7.85 (d, 2H, H<sub>d</sub>), 8.20 (d, 2H, H<sub>a</sub>), 8.89 (s, 1H, H<sub>e</sub>). <sup>13</sup>C NMR (DMSO-*d*<sub>6</sub>, δ, ppm): 120.9 (C<sup>3</sup>), 122.1 (C<sup>2</sup>), 126.9 (C<sup>5</sup>), 129.1 (C<sup>6</sup>), 130.1 (C<sup>4</sup>), 130.7 (C<sup>7</sup>), 131.4 (C<sup>8</sup>), 143.7 (C<sup>1</sup>).



### 9-Aminoanthracene (2)

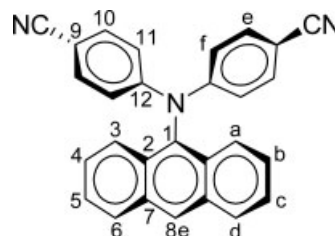
In a 500-mL three-neck round-bottomed flask equipped with a stirring bar under nitrogen atmosphere, 12.00 g (53.74 mmol) of nitro compound **1** and 0.68 g of 10% Pd/C were dissolved/suspended in 260 mL of ethanol. The suspension solution was heated to reflux, and 3 mL of hydrazine monohydrate was added slowly to the mixture, then the solution was stirred at reflux temperature. After a further 12 h of reflux, the solution was filtered to remove Pd/C, and the filtrate was cooled to precipitate yellow crystals. The product was collected by filtration and dried *in vacuo* at 80 °C to give 9.49 g (91% in yield) of yellow crystals with mp of 163–165 °C (lit.<sup>19</sup> 120–123 °C). FTIR (KBr): 3411, 3490 cm<sup>-1</sup> (–NH<sub>2</sub> stretch). <sup>1</sup>H NMR (DMSO-*d*<sub>6</sub>, δ, ppm): 7.28 (t, 2H, H<sub>c</sub>), 7.37 (t, 2H, H<sub>b</sub>), 7.61 (s, 1H, H<sub>e</sub>), 7.83 (d, 2H, H<sub>d</sub>), 8.33 (d, 2H, H<sub>a</sub>), 6.61 (s, 2H, NH<sub>2</sub>). <sup>13</sup>C NMR (DMSO-*d*<sub>6</sub>, δ, ppm): 112.2 (C<sup>3</sup>), 116.9 (C<sup>2</sup>), 122.3

(C<sup>4</sup>), 123.3 (C<sup>5</sup>), 125.5 (C<sup>6</sup>), 128.2 (C<sup>8</sup>), 132.4 (C<sup>7</sup>), 141.5 (C<sup>1</sup>).



### 9-[N,N-Di(4-cyanophenyl)amino]anthracene (3)

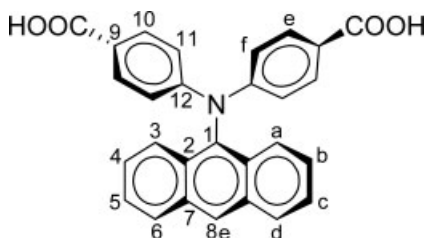
A mixture of 1.46 g (57.8 mmol) of sodium hydride and 75 mL of DMF was stirred at room temperature for 30 min. To the mixture, 4.82 g (24.9 mmol) of 9-aminoanthracene and 6.36 g (52.0 mol) of 4-fluorobenzonitrile were added in sequence. The mixture was heated with stirring at 160 °C for 15 h under nitrogen and then precipitated into 1000 mL of water/methanol (1:1). The product was filtered and recrystallized from acetonitrile (CH<sub>3</sub>CN) to afford 7.72 g (78% in yield) of light green lepto-slice with mp of 253–254 °C (by DSC). IR (KBr): 2223 cm<sup>-1</sup> (C=N stretch). <sup>1</sup>H NMR (DMSO-*d*<sub>6</sub>, δ, ppm): 7.12 (d, 4H, H<sub>g</sub>), 7.51–7.59 (m, 4H, H<sub>b</sub>+H<sub>c</sub>), 7.66 (d, 4H, H<sub>f</sub>), 7.89 (d, 4H, H<sub>d</sub>), 8.25 (d, 2H, H<sub>a</sub>), 8.86 (s, 1H, H<sub>e</sub>). <sup>13</sup>C NMR (DMSO-*d*<sub>6</sub>, δ, ppm): 104.2 (C<sup>9</sup>), 119.1 (–C=N), 120.6 (C<sup>11</sup>), 122.6 (C<sup>6</sup>), 126.2 (C<sup>4</sup>), 128.4 (C<sup>5</sup>), 129.0 (C<sup>8</sup>), 129.5 (C<sup>2</sup>), 129.6 (C<sup>3</sup>), 132.4 (C<sup>7</sup>), 134.0 (C<sup>1</sup>), 134.1 (C<sup>10</sup>), 149.7 (C<sup>12</sup>). Anal. Calcd. (%) for C<sub>28</sub>H<sub>17</sub>N<sub>3</sub> (395.45): C, 85.04; H, 4.33; N, 10.63. Found: C, 85.02; H, 4.18; N, 10.49.



### 9-[N,N-Di(4-carboxyphenyl)amino]anthracene (4)

A mixture of 4.35 g (77.5 mol) of potassium hydroxide and 1.88 g (4.75 mmol) of the obtained dinitrile compound **3** in 20 mL of ethanol and 30 mL of distilled water was stirred at ~ 100 °C until no further ammonia was generated. The time taken to reach this stage was about 5 days. The solution was cooled and filtered, and the pH value was adjusted by dilute hydrochloric acid to near 3. The light yellow-green precipitate was filtered, washed thoroughly with water and recrystallized from ethanol to afford 1.80 g (87% in

yield) of yellow-green crystals with mp of 338–339 °C (by DSC). IR (KBr): 1686 (C=O stretch), 2700–3200  $\text{cm}^{-1}$  (O–H stretch).  $^1\text{H}$  NMR (DMSO- $d_6$ ,  $\delta$ , ppm): 7.07 (d, 4H,  $\text{H}_g$ ), 7.45–7.54 (m, 4H,  $\text{H}_b + \text{H}_c$ ), 7.81 (d, 4H,  $\text{H}_f$ ), 7.94 (d, 2H,  $\text{H}_d$ ), 8.21 (d, 2H,  $\text{H}_a$ ), 8.79 (s, 1H,  $\text{H}_e$ ), 12.66 (s, 2H, OH).  $^{13}\text{C}$  NMR (DMSO- $d_6$ ,  $\delta$ , ppm): 119.7 ( $\text{C}^{11}$ ), 123.1 ( $\text{C}^6$ ), 124.2 ( $\text{C}^9$ ), 126.1 ( $\text{C}^4$ ), 128.0 ( $\text{C}^5$ ), 128.4 ( $\text{C}^8$ ), 129.5 ( $\text{C}^3$ ), 129.7 ( $\text{C}^2$ ), 131.4 ( $\text{C}^{10}$ ), 132.5 ( $\text{C}^7$ ), 135.2 ( $\text{C}^1$ ), 150.3 ( $\text{C}^{12}$ ), 167.0 (C=O). Anal. Calcd (%) for  $\text{C}_{28}\text{H}_{19}\text{NO}_4$  (433.45): C, 77.59; H, 4.42; N, 3.23. Found: C, 77.59; H, 4.39; N, 3.20.

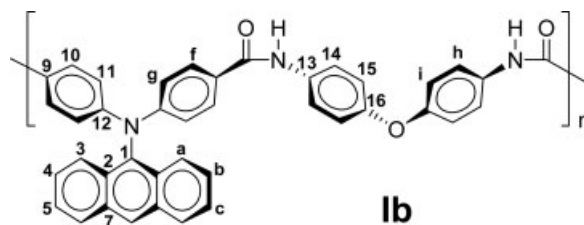


### Polymer Synthesis

The synthesis of polyamide **1b** was used as an example to illustrate the general synthetic route used to produce the poly(amine-amide)s. A mixture of 0.217 g (0.5 mmol) of dicarboxylic acid, 9-[*N,N*-di(4-carboxyphenyl)amino]anthracene (**4**), 0.100 g (0.5 mmol) of 4,4'-oxydianiline (**5b**), 0.06 g of calcium chloride, 0.5 mL of triphenyl phosphite, 0.25 mL of pyridine, and 0.5 mL of NMP was heated with stirring at 105 °C for 3 h. The obtained polymer solution was poured slowly into 300 mL of stirred methanol giving rise to a stringy, fiber-like precipitate that was collected by filtration, washed thoroughly with hot water and methanol, and dried under vacuum at 100 °C. Precipitations from DMAc into methanol were carried out twice for further purification. The inherent viscosity and weight-average molecular weights ( $M_w$ ) of the obtained polyamide **1b** was 0.44 dL/g (measured at a concentration of 0.5 g/dL in DMAc at 30 °C) and 42,400 Da, respectively.  $^1\text{H}$  NMR (DMSO- $d_6$ ,  $\delta$ , ppm): 6.95 (d, 4H,  $\text{H}_h$ ), 7.09 (d, 4H,  $\text{H}_g$ ), 7.50–7.58 (m, 4H,  $\text{H}_b + \text{H}_c$ ), 7.69 (d, 4H,  $\text{H}_i$ ), 7.81 (d, 4H,  $\text{H}_f$ ), 7.98 (d, 2H,  $\text{H}_d$ ), 8.24 (d, 2H,  $\text{H}_a$ ), 8.82 (s, 1H,  $\text{H}_e$ ), 10.08 (amide–NH).  $^{13}\text{C}$  NMR (DMSO- $d_6$ ,  $\delta$ , ppm): 118.8 ( $\text{C}^{14}$ ), 119.6 ( $\text{C}^{11}$ ), 120.7 ( $\text{C}^9$ ), 122.2 ( $\text{C}^{15}$ ), 123.3 ( $\text{C}^6$ ), 126.1 ( $\text{C}^4$ ), 128.0 ( $\text{C}^5$ ), 128.4 ( $\text{C}^{2+8}$ ), 129.7 ( $\text{C}^{3+10}$ ), 132.5 ( $\text{C}^7$ ), 135.1 ( $\text{C}^{13}$ ), 135.5 ( $\text{C}^1$ ), 149.5 ( $\text{C}^{16}$ ), 153.0 ( $\text{C}^{12}$ ), 165.0 (amide carbonyl). Anal. Calcd. For  $(\text{C}_{40}\text{H}_{27}\text{N}_3\text{O}_3)_n$  (597.66) $_n$ : C, 80.38%; H, 4.55%; N, 7.03%. Found: C, 80.25%; H, 4.62%; N, 7.10%.

*Journal of Polymer Science: Part A: Polymer Chemistry*  
DOI 10.1002/pola

The other polyamides were prepared by an analogous procedure.

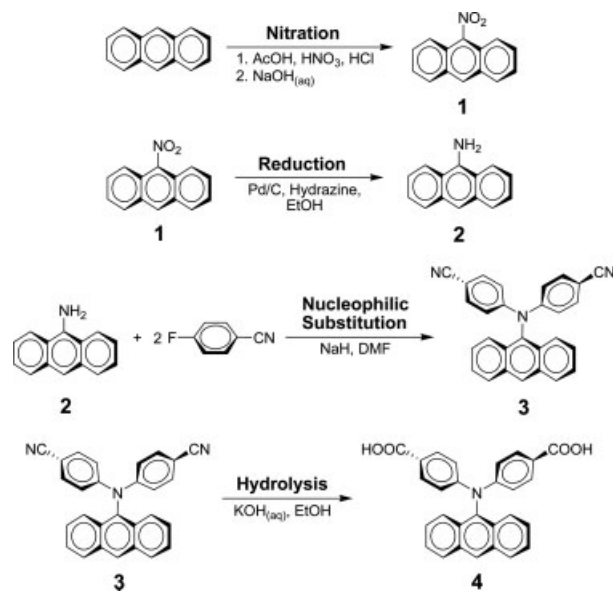


### Preparation of the Polyamide Films

A solution of polymer was made by dissolving about 0.35 g of the polyamides sample in 6 mL of DMAc. The homogeneous solution was poured into a 5-cm glass Petri dish, which was heated at 40 °C for 4 h, 100 °C for 2 h, and 160 °C for 6 h to slowly release the solvent under vacuum. The obtained films were about 45–70  $\mu\text{m}$  in thickness and were used for X-ray diffraction measurements, solubility tests, thermal analyses, optical and electrochemical properties measurements.

### Measurements

Fourier transform infrared (FTIR) spectra were recorded on a PerkinElmer RXI FTIR spectrometer. Elemental analyses were run in a VarioEL-III Elemental.  $^1\text{H}$  and  $^{13}\text{C}$  nuclear magnetic resonance (NMR) spectra were measured on a Bruker AV-300 FT NMR system and referenced to the DMSO- $d_6$  signal, and peak multiplicity was reported as follows: s, singlet; d, doublet; t, triplet; m, multiplet. The inherent viscosities were determined at 0.5 g/dL concentration using Tamson TV-2000 viscometer at 30 °C. Molecular weight and molecular weight distributions were determined through gel permeation chromatography (GPC) at 50 °C using a Waters 510 HPLC, equipped with a 410 differential refractometer, a refractive index (RI) detector, and an UV detector. Three Ultrastaygel columns (100, 500, and 10 $^3$ ) were connected in series in order of increasing pore size, with DMF as eluent at a flow rate of 0.6 mL/min. Wide-angle X-ray diffraction (WAXD) measurements were performed at room temperature ( $\sim 25$  °C) on a Shimadzu XRD-7000 X-ray diffractometer (40 kV, 20 mA), using graphite-monochromatized Cu-K $\alpha$  radiation. The molecular weight calibration curve was obtained using polystyrene standards. Thermogravimetric analysis (TGA) was conducted with a PerkinElmer Pyris 1 TGA. Experiments were carried out on  $\sim 6$ –8 mg



Scheme 1. Monomer synthesis.

film samples heated in flowing nitrogen or air (flow rate: 20 cm<sup>3</sup>/min) at a heating rate of 20 °C/min. Thermomechanical analysis (TMA) was conducted with a PerkinElmer Diamond TMA instrument. The TMA experiments were conducted from 50 to 350 °C at a scan rate of 10 °C/min with a penetration probe 1.0 mm in diameter under an applied constant load of 50 mN. Softening temperatures ( $T_s$ ) were taken as the onset temperatures of probe displacement on the TMA traces. Ultraviolet-visible (UV-vis) spectra of the polymer films were recorded on a Varian Cary 50 Probe spectrometer. Photoluminescence (PL) spectra were measured with a Jasco FP-6300 spectrofluorometer. PL quantum yields ( $\Phi_{PL}$ ) of the samples in different solvents were measured by using quinine sulfate dissolved in 1 N sulfuric acid as a reference standard ( $\Phi_{PL} = 0.546$ ).<sup>20</sup> The Photoluminescence quantum yields (PLQYs) of polymer thin films were determined using a calibrated integrating sphere coupled to a charge coupled device (CCD) spectrograph. The 325-nm line of the He-Cd laser was used to excite samples placed in the calibrated integrating sphere. All spectra were obtained by averaging five scans. Cyclic voltammetry (CV) was performed with a Bioanalytical System Model CV-27 potentiostat and a BAS X-Y recorder with ITO (polymer films area about 0.7 cm × 0.5 cm) was used as a working electrode and a platinum wire as an auxiliary electrode at a scan rate of 50 and 100 mV/s against a Ag/AgCl reference electrode in dry acetonitrile (CH<sub>3</sub>CN) and *N,N*-dimethylformamide (DMF) solution of

0.1 M tetrabutylammonium perchlorate (TBAP) under nitrogen atmosphere for oxidation and reduction measurements, respectively. Voltammograms are presented with the positive/negative potential pointing to the right/left with increasing anodic/decreasing cathodic current pointing upwards/downwards.

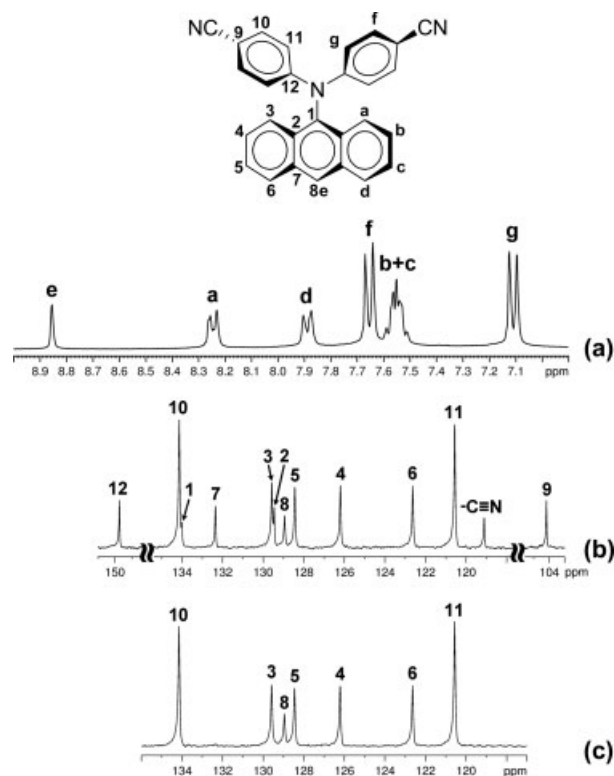
## RESULTS AND DISCUSSION

### Monomer Synthesis

The synthesis procedure of diacid monomer and three intermediate compounds is outlined in Scheme 1. 9-Nitroanthracene (1) was synthesized by the electrophilic aromatic substitution reaction between anthracene and nitric acid. The 9-aminoanthracene (2) could be obtained by Pd/C-catalytic reduction of compound 1 with hydrazine monohydrate under a nitrogen atmosphere. The new aromatic dicarboxylic acid having bulky pendent anthrylamine group, 9-[*N,N*-di(4-carboxyphenyl)amino]anthracene (4), was successfully synthesized by the double *N*-arylation reaction of 9-aminoanthracene with 4-fluorobenzonitrile in DMF in the presence of sodium hydride as a base, followed by the alkaline hydrolysis of the intermediate dinitrile compound (3). Elemental analysis, IR, and <sup>1</sup>H and <sup>13</sup>C NMR spectroscopic techniques were used to identify structures of the intermediate compound 1, 2, dinitrile compound 3, and dicarboxylic acid monomer 4. The FTIR spectrum of compounds 3 showed nitrile characteristic band at 2223 cm<sup>-1</sup> (C=N stretching). After hydrolysis, the characteristic absorptions of the diacid exhibited the typical C=O and O-H stretching absorptions at 1676 and 2700–3200 cm<sup>-1</sup>, respectively. Figures 1 and 2 illustrate the <sup>1</sup>H NMR and <sup>13</sup>C NMR spectra of dinitrile compound 3, and dicarboxylic acid monomer 4, respectively. Assignments of each carbon and proton are assisted by the two-dimensional H-H COSY (Correlation Spectroscopy) and C-H HMQC (Heteronuclear Multiple Quantum Correlation) spectra given in Figures 3 and 4, and these spectra agree well with the proposed molecular structure of dicarboxylic acid monomer 4.

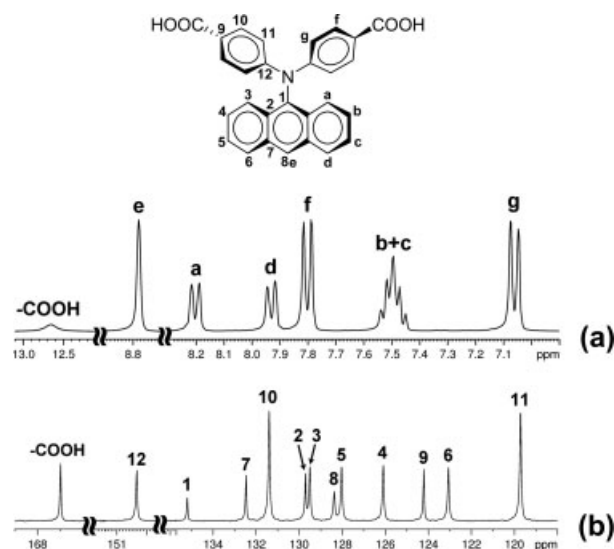
### Polymer Synthesis

According to the phosphorylation technique first described by Yamazaki and coworkers,<sup>21</sup> a series of novel polyamides (I) with pendent anthrylamine units were synthesized from the

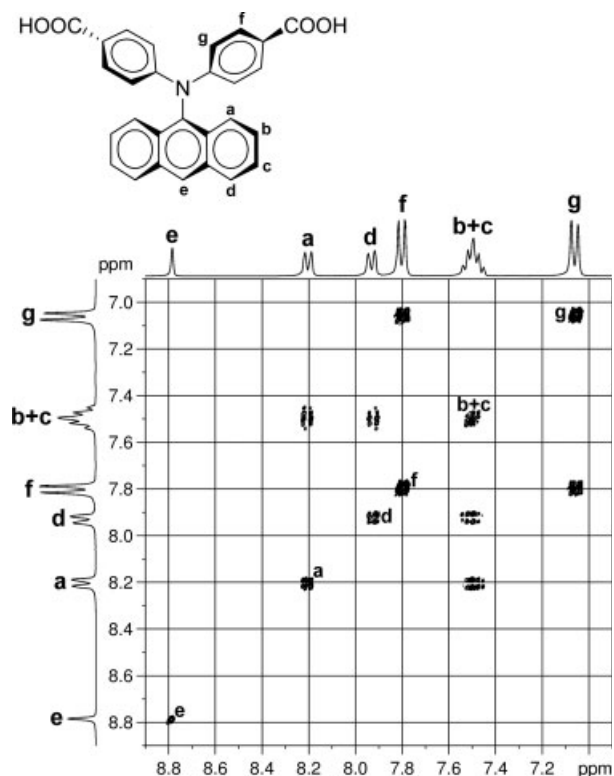


**Figure 1.** (a)  $^1\text{H}$  NMR, (b)  $^{13}\text{C}$  NMR and (c) DEPT-135 spectra of dinitrile compound **3** in  $\text{DMSO-}d_6$ .

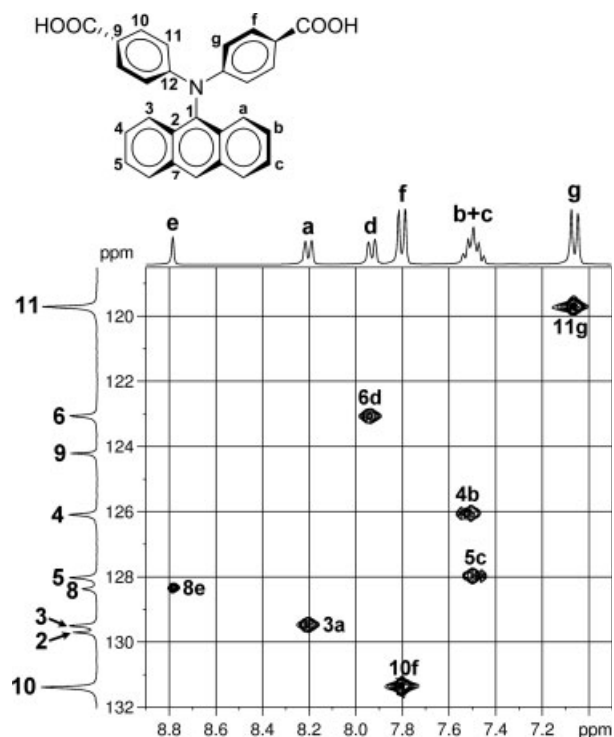
dicarboxylic acid, 9-[*N,N*-di(4-carboxyphenyl)amino]anthracene (**4**), and various aromatic diamines (**5**) as shown in Scheme 2. The polymerization was carried out via solution polycondensation



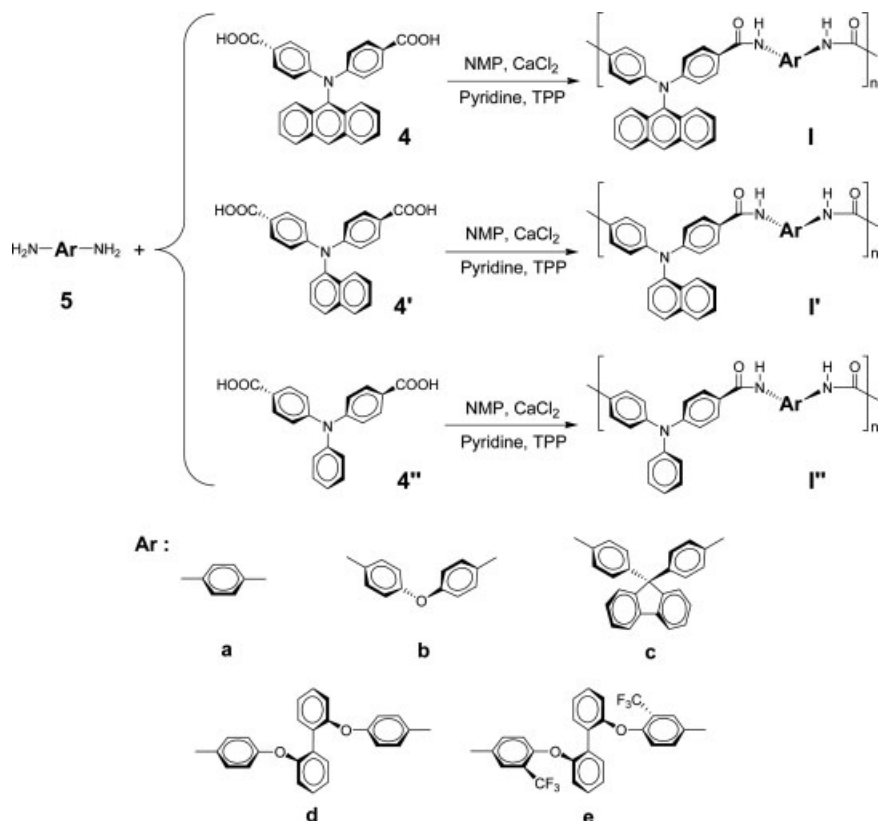
**Figure 2.** (a)  $^1\text{H}$  NMR and (b)  $^{13}\text{C}$  NMR spectra of diacid monomer **4** in  $\text{DMSO-}d_6$ .



**Figure 3.** H-H COSY spectrum of diacid monomer **4** in  $\text{DMSO-}d_6$ .



**Figure 4.** C-H HMQC spectrum of diacid monomer **4** in  $\text{DMSO-}d_6$ .



**Scheme 2.** Synthesis of aromatic poly(amine-amide)s.




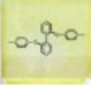
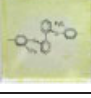
using triphenyl phosphite and pyridine as condensing agents. The polymerization proceeded homogeneously throughout the reaction and afforded clear, viscous polymer solutions. All the polymers precipitated in a tough fiber-like form when slowly pouring the resulting polymer solutions into methanol. The obtained polyamides had inherent viscosities in the range of 0.18–0.51 dL/g with weight-average molecular weights ( $M_w$ ) and degree of polymerization (DP) in the range of 34,100–43,500 Da and 24.0–40.4, respectively, relative to polystyrene standards (Table 1). The formation of the polyamides was confirmed with IR and NMR spectroscopy. IR spectrum for polyamide **Ib** in Figure 5 exhibited characteristic absorption bands of the amide group around 3408 (N–H stretching), 1655  $\text{cm}^{-1}$  (amide carbonyl). Figure 6 shows a typical set of  $^1\text{H}$  and  $^{13}\text{C}$  NMR spectra of polyamide **Ib** in  $\text{DMSO-}d_6$ , where all the peaks were consistent with the expected structure. Assignments of each carbon and proton are assisted by the two-dimensional C–H HMQC spectrum shown in Figure 7, and these spectra agree well with the proposed molecular structure of polyamide **Ib**.

## Polymer Properties

### Basic Characterization

The solubility behavior of aromatic polyamides **I** was tested qualitatively and the results are summarized in Table 2. All polymers exhibited good solubility in variety solvents such as NMP, DMAc, DMF, and DMSO. It is noted the polyamide **Ia** obtained from rigid *p*-phenylenediamine monomer (**5a**) was also could be soluble in NMP and DMAc. Furthermore, polyamides **Id** and **Ie** were soluble in *m*-cresol and THF. The enhanced solubility can be attributed to the introduction of bulky, asymmetrical and kinked 9-anthryldiphenylamine structure into the repeat unit, which decreases interchain interactions and increases the free volume. Thus, the excellent solubility makes these polymers as potential candidates for practical applications by spin- or dip-coating processes. Furthermore, the wide-angle X-ray diffraction diagram (WAXD) patterns of these anthrylamine-based polyamide films revealed amorphous nature, which also was reflected in their excellent solubility observed.

**Table 1.** Inherent Viscosity and Molecular Weights. [Color table can be viewed in the online issue, which is available at [www.interscience.wiley.com](http://www.interscience.wiley.com).]

Polymer	$\eta_{inh}^a$ (dL/g)	Color of Film <sup>b</sup>	$M_w^c$	$M_n^c$	PDI <sup>d</sup>	DP <sup>e</sup>
Ia	0.51		38,600	20,500	1.88	40.4
Ib	0.44		42,400	20,600	2.06	34.4
Ic	0.32		43,500	22,600	1.92	30.2
Id	0.25		34,100	19,000	1.79	24.7
Ie	0.18		36,200	21,700	1.67	24.0

<sup>a</sup> Measured at a polymer concentration of 0.5 g/dL in DMAc at 30 °C.

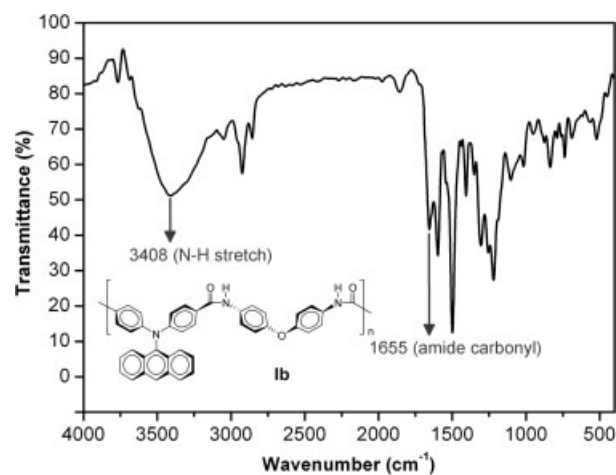
<sup>b</sup> The photographs are the appearance of the polymer films (thickness: 1–3  $\mu$ m).

<sup>c</sup> Calibrated with polystyrene standards, using DMF as the eluent at a constant flow rate of 1 mL/min at 50 °C.

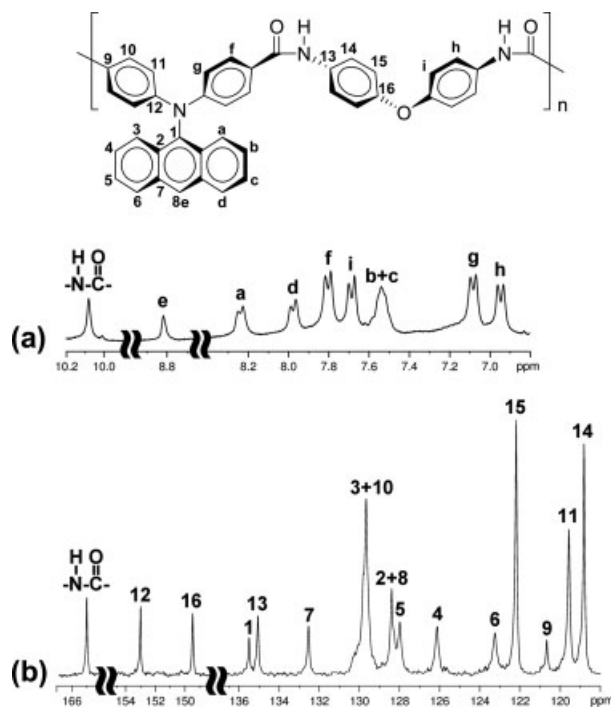
<sup>d</sup> Polydispersity index ( $M_w/M_n$ ).

<sup>e</sup> Degree of polymerization.

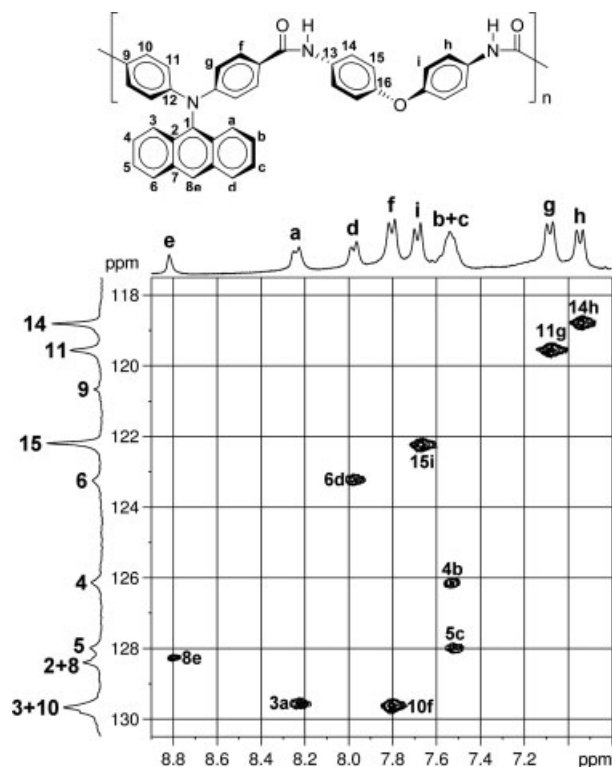
The thermal properties of the polyamides were investigated by TGA and TMA. Typical TGA and TMA thermograms of a representative polyamide **Id** is illustrated in Figure 8. All the aromatic polyamides exhibited good thermal stability with in-



**Figure 5.** IR spectrum of polyamide **Ib** film.



**Figure 6.** (a)  $^1\text{H}$  NMR and (b)  $^{13}\text{C}$  NMR spectra of polyamide **Ib** in  $\text{DMSO-}d_6$ .



**Figure 7.** C-H HMQC spectrum of polyamide **Ib** in  $\text{DMSO-}d_6$ .



Table 2. Solubility Behavior

Solubility in Various Solvents <sup>a</sup>										
Code	NMP	DMAc	DMF	DMSO	<i>m</i> -Cresol	THF	CHCl <sub>3</sub>	Toluene		
Ia	++ (+++) <sup>b</sup> [++] <sup>c</sup>	++ (+) [+-]	++ (+) [+-]	++ (+) [+-]	++ (+) [+-]	++ (+) [+-]	++ (+) [+-]	++ (+) [+-]	++ (+) [+-]	++ (+) [+-]
Ib	++ (+) [++]	++ (+) [++]	++ (+) [++]	++ (+) [++]	++ (+) [++]	++ (+) [++]	++ (+) [++]	++ (+) [++]	++ (+) [++]	++ (+) [++]
Ic	++ (+) [++]	++ (+) [++]	++ (+) [++]	++ (+) [++]	++ (+) [++]	++ (+) [++]	++ (+) [++]	++ (+) [++]	++ (+) [++]	++ (+) [++]
Id	++ (+) [++]	++ (+) [++]	++ (+) [++]	++ (+) [++]	++ (+) [++]	++ (+) [++]	++ (+) [++]	++ (+) [++]	++ (+) [++]	++ (+) [++]
Ie	++ (+) [++]	++ (+) [++]	++ (+) [++]	++ (+) [++]	++ (+) [++]	++ (+) [++]	++ (+) [++]	++ (+) [++]	++ (+) [++]	++ (+) [++]

+ +, Soluble at room temperature; +, soluble on heating; -, partially soluble or swelling; -, insoluble even on heating.

<sup>a</sup>The solubility was determined with a 1 mg sample in 1 mL of a solvent.

<sup>b</sup>Data in parentheses are polyamides I' series.

<sup>c</sup>Data in parentheses are polyamides I'' series.

significant weight loss up to 500 °C in nitrogen. The 10% weight-loss temperatures ( $T_d^{10}$ ) of the aromatic polyamides in nitrogen and air were recorded in the range of 545–560 and 500–565 °C, respectively, as summarized in Table 3. The amount of carbonized residue (char yield) of these polymers in nitrogen atmosphere was more than 62% at 800 °C. The high char yields of these polymers can be ascribed to their high aromatic content. The softening temperatures ( $T_s$ ) of the polymer film samples were determined by the TMA method with a loaded penetration probe. They were obtained from the onset temperature of the probe displacement on the TMA traces. In addition, when compared with the analogous polyamides I' and I'', the I series showed a higher  $T_s$  and better thermal stability as shown in Table 3 due to the introduction of more bulky and hindered rotation aromatic anthracene unit into the triarylamine structure.

### Optical Properties

The optical properties of the polyamides were investigated by UV-vis and photoluminescence spectroscopy. The results are summarized in Table 4. These polymers exhibited maximum UV-vis absorption at 348–360 nm in NMP solutions as shown in Figure 9, due to the  $\pi$ - $\pi^*$  transitions of the aromatic chromophores, anthracene and triarylamine units. The photophysical behavior for film specimens of anthrylamine-based polyamides I revealed nearly identical results as solution state with a single absorbance at 349–359 nm. Figure 9 also shows the PL spectra of polyamides I measured in NMP (Conc.:  $10^{-6}$  mol/L). The quantum yields of these polymers after refractive

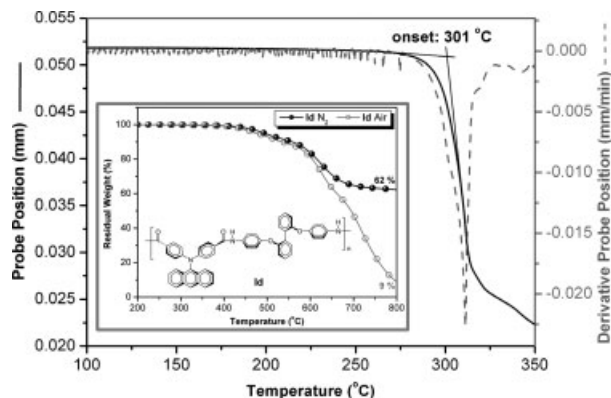


Figure 8. TGA thermograms and TMA traces of polyamide Id.

**Table 3.** Thermal Behavior

Polymer <sup>a</sup>	$T_s$ (°C) <sup>b</sup>	$T_d^5$ (°C) <sup>c</sup>		$T_d^{10}$ (°C) <sup>d</sup>		Char Yield (wt %) <sup>e</sup>
		N <sub>2</sub>	Air	N <sub>2</sub>	Air	
<b>Ia</b>	299	495	480	555	535	69
<b>Ib</b>	288	500	490	545	525	70
<b>Ic</b>	301	505	490	545	565	68
<b>Id</b>	301	495	475	560	535	62
<b>Ie</b>	290	480	450	545	500	68
<b>I'a</b>	298	490	480	550	530	66
<b>I'b</b>	288	485	465	540	555	67
<b>I'c</b>	297	500	500	540	565	70
<b>I''a</b>	298	480	475	520	530	68
<b>I''b</b>	283	450	445	500	495	64
<b>I''c</b>	293	490	500	545	560	69

<sup>a</sup>The polymer film samples were heated at 300 °C for 1 h prior to all the thermal analyses.

<sup>b</sup>Softening temperature measured by TMA with a constant applied load of 50 mN at a heating rate of 10 °C/min.

<sup>c</sup>Temperature at which 5 % weight loss occurred, recorded via TGA at a heating rate of 20 °C/min and a gas-flow rate of 20 cm<sup>3</sup>/min.

<sup>d</sup>Temperature at which 10 % weight loss occurred.

<sup>e</sup>Residual weight percentage at 800 °C in nitrogen.

index correction can be calculated according to eq 1<sup>22</sup>:

$$\phi_{\text{unk}} = \phi_{\text{std}} \left( \frac{I_{\text{unk}}}{I_{\text{std}}} \right) \left( \frac{A_{\text{std}}}{A_{\text{unk}}} \right) \left( \frac{\eta_{\text{unk}}}{\eta_{\text{std}}} \right)^2 \quad (1)$$

where  $\phi_{\text{unk}}$ ,  $\phi_{\text{std}}$ ,  $I_{\text{unk}}$ ,  $I_{\text{std}}$ ,  $A_{\text{unk}}$ ,  $A_{\text{std}}$ ,  $\eta_{\text{unk}}$ , and  $\eta_{\text{std}}$  are the fluorescent quantum yield, integration of

the emission intensity, absorbance at the excitation wavelength, and the refractive indices of the corresponding solutions for the samples and the standard, respectively. Here, we use the refractive indices of the pure solvents as those of the solutions. The aromatic polyamides **I** series exhibited PL emission maxima around 487–492 nm in NMP solution with high PL quantum yield ranging from

**Table 4.** Optical Properties

Index [a]	NMP (1 × 10 <sup>-6</sup> M) Solution, R.T.			Film (nm), R.T.			
	$\lambda_{\text{abs}}$ (nm)	$\lambda_{\text{em}}$ (nm) <sup>a</sup>	$\Phi_{\text{PL}}$ (%) <sup>b</sup>	$\lambda_0^c$	$\lambda_{\text{abs}}$	$\lambda_{\text{onset}}$	$\lambda_{\text{em}}^a$
<b>Ia</b>	360	492	55.2 (nd) <sup>d</sup>	433	359	395	484
<b>Ib</b>	350	490	57.8 (2)	431	352	388	482
<b>Ic</b>	351	490	69.3 (3)	429	350	388	483
<b>Id</b>	348	491	68.5 (2)	427	349	387	483
<b>Ie</b>	350	487	73.9 (6)	423	350	386	478
<b>I'a</b>	362	458	1.3	401	356	401	468
<b>I'b</b>	350	425	4.9	390	358	396	444
<b>I'c</b>	350	422	15.0	390	356	392	440
<b>I''a</b>	366	458	1.2	404	366	404	454
<b>I''b</b>	354	428	3.2	393	361	397	450
<b>I''c</b>	353	428	10.4	395	360	398	449

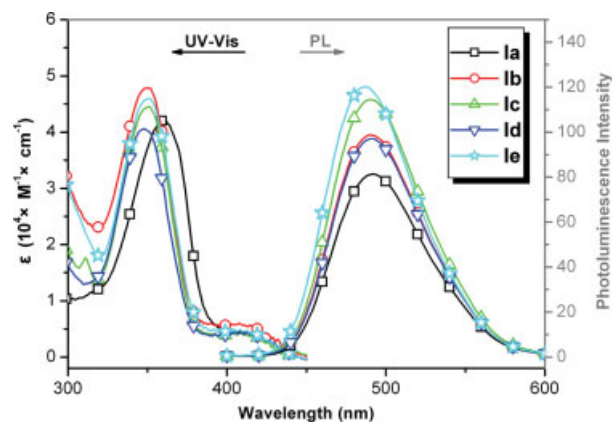
nd, Not been measured.

<sup>a</sup>They were excited at  $\lambda_{\text{abs}}$  for both solid and solution states.

<sup>b</sup>The quantum yield was measured by using quinine sulfate (dissolved in 1 N H<sub>2</sub>SO<sub>4</sub> with a concentration of 10<sup>-5</sup> M, assuming photoluminescence quantum efficiency of 0.546) as a standard at 24–25 °C.

<sup>c</sup>The cutoff wavelength from the UV-vis transmission spectra of polymer films (thickness: 1–3 μm).

<sup>d</sup>Data in parentheses are the PLQYs of polymer thin films determined using a calibrated integrating sphere.

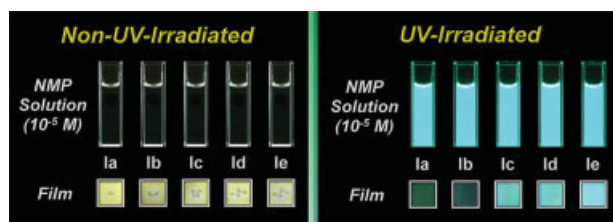


**Figure 9.** Molar absorptivity ( $\epsilon$ ) and photoluminescence (PL) spectra of polyamides **I** in NMP solution ( $10^{-6}$  M).

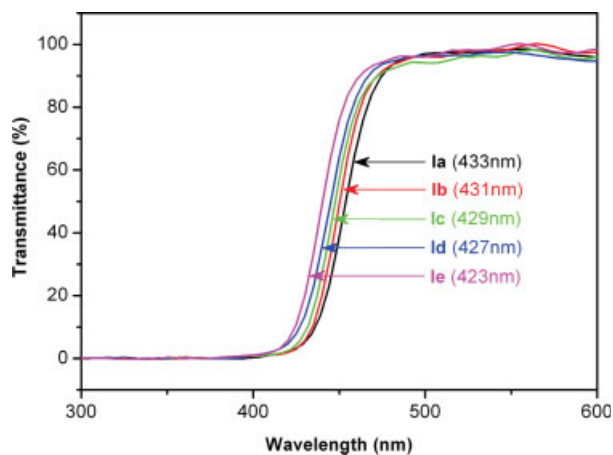
55.2% for **Ia** to 73.9% for **Ie**, and exhibited PLQYs ranged from 2 to 6% in film states. Comparing the optical properties data of polyamides bearing aniline, naphthylamine, anthrylamine, and carbazole,<sup>9(b)</sup> we found that the PL quantum yield of series **I** is superior than all of the other series. It means that the anthrylamine chromophores are more effectively improving the photoluminescence in the prepared polyamides. To the best of our knowledge, polymer **Ie** shows the highest PL quantum yield within wholly aromatic polyamide system, and the PL behavior for solutions and thin films of the polyamides **I** by UV irradiation is summarized in Figure 10. The cutoff wavelengths (absorption edge;  $\lambda_0$ ) of polyamide films, measured by transmission UV-vis spectra as shown Figure 11, were in the range of 423–433 nm with light-color and high optical transparency.

### Solvatochromism

The absorption and PL spectra of the solutions of polyamide **Ie** in various solvents with its thin film

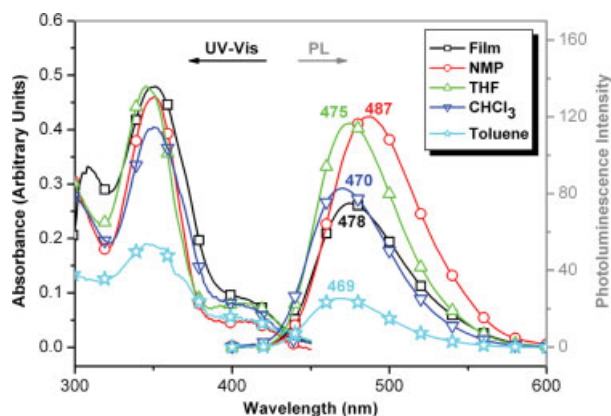


**Figure 10.** The photoluminescence of polyamide solutions ( $10^{-5}$  M) and thin films (thickness: 1–3  $\mu\text{m}$ ) by UV irradiation (Excited at 365 nm).

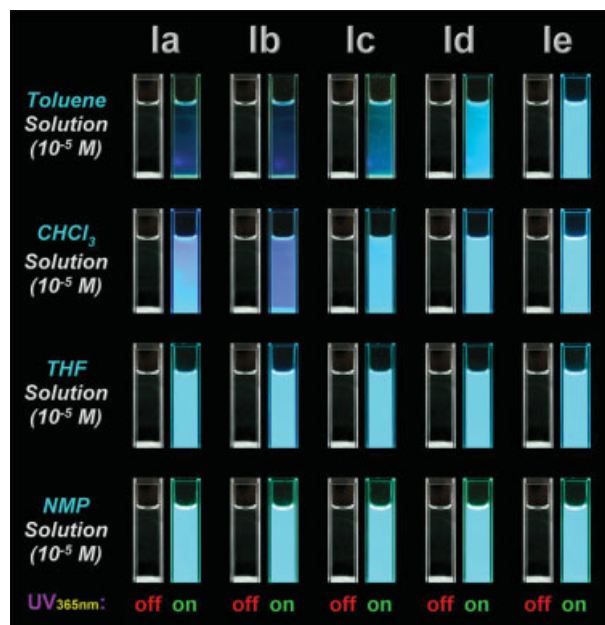


**Figure 11.** UV-visible transmission spectra of polyamide films (thickness: 1–3  $\mu\text{m}$ ).

was shown in Figure 12. The absorption spectra of polyamide **Ie** in four different solvents were very similar to each other, while the PL spectrum progressively shifted to red with an increase in the solvent polarity, and PL emission maxima moving from 469 to 487 nm when the solvent is changed from toluene to NMP. Even more, the PL emission of polymer **Ie** in NMP was red-shifted compared to that of its thin solid film. The emission color changes from bluish green in toluene to green in NMP when the polymer **I** solutions were illuminated under a 365-nm UV lamp (Fig. 13), which well coincided with their PL spectra. This result suggests that solvent-induced aggregation seems to simulate solid behavior in these polymer



**Figure 12.** UV-vis absorption and PL spectra of polyamide **Ie** in different solvents: Toluene, THF,  $\text{CHCl}_3$  and NMP (solution concentration is  $10^{-6}$  M and excited with  $abs_{\text{max}}$  respectively) with its thin film (thickness: 1–3  $\mu\text{m}$ ).



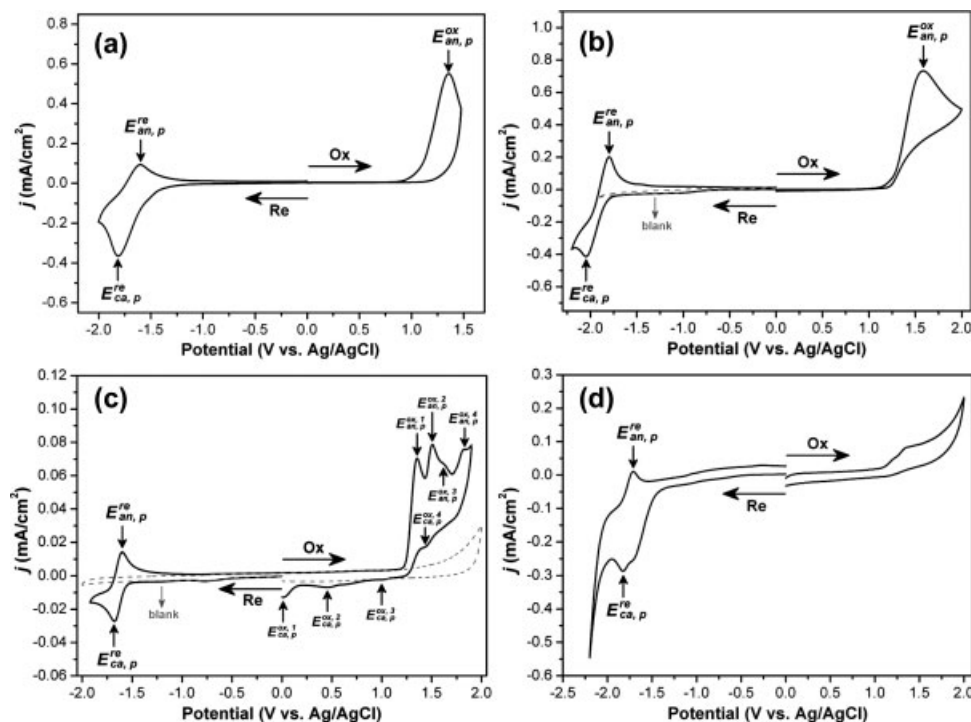
**Figure 13.** The photoluminescence of polyamide **I** in different solvent: Toluene, THF,  $\text{CHCl}_3$  and NMP ( $10^{-5}$  M) by UV irradiation (Excited at 365 nm). [Color figure can be viewed in the online issue, which is available at [www.interscience.wiley.com](http://www.interscience.wiley.com)]

**Table 5.** Photophysical Properties of **Ie** in Different Solvents<sup>a</sup>

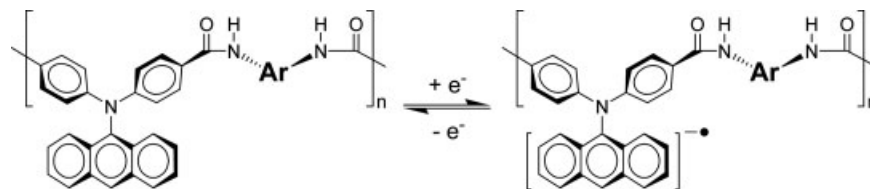
Solvent	$\lambda_{\text{abs}}$ (nm)	$\lambda_{\text{em}}$ (nm)	$\Phi_{\text{PL}}$ (%)
Toluene	345	469	32.6
$\text{CHCl}_3$	350	470	52.4
THF	346	475	60.0
NMP	350	487	73.9

<sup>a</sup> Polymer concentration of  $10^{-6}$  M in different solvents.

films excited states. The emission maxima increased dramatically as the medium changing from less polar (Toluene) to polar (NMP), and the solvatochromic shifts of the emission spectra are much larger than those of absorption spectra implying that the excited-state energy levels are influenced more than those in the electronic ground state.<sup>23</sup> The quantum efficiency of polymer **Ie** decreased with the decreasing polarity of solvent (Table 5) which was also previously reported in our laboratory.<sup>24</sup>



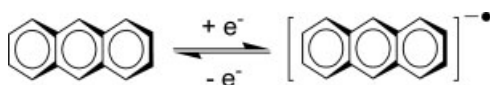
**Figure 14.** Cyclic voltammograms of (a) polyamide **Ia** film onto an indium-tin oxide (ITO)-coated glass substrate,  $10^{-3}$  M (b) anthracene, (c) dinitrile compound **3**, and (d) diacid monomer **4** in  $\text{CH}_3\text{CN}$  (oxidation) and DMF (reduction) solutions containing 0.1 M TBAP at scan rate of 50 and 100 mV/s, respectively.



**Scheme 3.** Reaction scheme for the electrochemical reduction of poly(amine-amide)s in an aprotic medium.

### Electrochemical Properties

The redox behavior of the polyamides **I** series was investigated by cyclic voltammetry (CV) conducted for the cast film on an ITO-coated glass substrate as working electrode in dry  $\text{CH}_3\text{CN}$  and DMF containing 0.1 M of TBAP as an electrolyte under nitrogen atmosphere for oxidation and reduction measurements, respectively. The electrochemical study for these polyamides undergoes one irreversible oxidation and one reversible reduction processes. The typical cyclic voltammograms for polyamide **Ia** are shown in Figure 14(a). The mechanism for the electrochemical reduction of poly(amine-amide)s could be depicted as in Scheme 3.<sup>25</sup> The electrochemical characteristics of anthracene [Fig. 14(b)], dinitrile compound **3** [Fig. 14(c)], and diacid monomer **4** [Fig. 14(d)] were compared with the polyamide **Ia** [Fig. 14(a)]. Anthracene showed reversibly reduced state in DMF ( $E_{\text{onset}} = -1.82$  V), and the mechanism for the electrochemical reduction is depicted as in Scheme 4.<sup>25</sup> After the double *N*-arylation reaction of 9-aminoanthracene, the dinitrile compound **3** and diacid monomer **4** exhibited reversible reduction processes at  $E_{\text{onset}} = -1.54$  and  $-1.48$  V, respectively, while the polyamides **Ia** exhibited reversible reduction processes at  $E_{1/2} = -1.52$  V. The reduction onset potential ( $E_{\text{onset}}$ ) of diacid monomer **4** was almost the same as those of the polyamides **I** ranging from  $-1.51$  to  $-1.54$  V. The energy levels of highest occupied molecular orbital (HOMO) and lowest unoccupied molecular orbital (LUMO) for these polyamides can be determined from the oxidation, reduction onset poten-



**Scheme 4.** Reaction scheme for the electrochemical reduction of anthracene in an aprotic medium.

tials ( $E_{\text{onset}}$ ) and the onset absorption wavelength,<sup>9(a)</sup> and the results are listed in Table 6. For example, the oxidation/reduction onset potential for polyamide **Ia** has been determined as 1.08/  $-1.52$  (V versus Ag/AgCl). The external ferrocene/ferrocenium ( $\text{Fc}/\text{Fc}^+$ ) redox standard  $E_{1/2}$  ( $\text{Fc}/\text{Fc}^+$ ) is 0.44 V versus Ag/AgCl in  $\text{CH}_3\text{CN}$ . Assuming that the HOMO energy for the  $\text{Fc}/\text{Fc}^+$  standard is 4.80 eV with respect to the zero vacuum level, the HOMO and LUMO energies for polymer **Ia** could be evaluated to be 5.44 and 2.84 eV, respectively.

### CONCLUSIONS

The newly triarylamine-containing aromatic dicarboxylic acid, 9-[*N,N*-di(4-carboxyphenyl)amino]anthracene (**4**) was successfully synthesized in high purity and good yields. A series of novel polyamides could be readily prepared from the dicarboxylic acid and various aromatic diamines via the direct phosphorylation polycondensation. The introduction of the bulky anthracene unit into the polymer backbone could effectively disrupt the coplanarity of aromatic units in chain packing which increases the between-chain space or free volume thus enhancing solubility and thermal stability of the obtained polyamides. All the amorphous polymers exhibited high optical transparency from UV-vis transmittance measurement with cutoff wavelength in the range of 423–433 nm, and exhibited green emission maximum around 478–484 nm in solid state. These polyamides exhibited highly photoluminescence quantum yield in NMP solution ranges from 55.2% for **Ia** to 73.9% for **Ie** due to the introduction of anthrylamine chromophores. Owing to their relatively high quantum efficiency, these novel anthrylamine-based polyamides could be considered as new candidates for organo-processable high-performance polymers for green-light-emitting materials.

**Table 6.** Electrochemical Properties

Index	Oxidation/V <sup>a</sup>	Reduction/V <sup>b</sup>		$E_g^{EC}$ (eV) <sup>c</sup>	$E_g^{Opt}$ (eV) <sup>d</sup>	$E_{HOMO}$ (eV) <sup>e</sup>	$E_{LUMO}$ (eV)
	$E_{onset}$	$E_{1/2}^f$	$E_{onset}$				
<b>Ia</b>	1.08	-1.71	-1.52	2.60	3.14	5.44	2.84
<b>Ib</b>	1.13	-1.71	-1.54	2.67	3.20	5.49	2.82
<b>Ic</b>	1.13	-1.70	-1.51	2.64	3.20	5.49	2.85
<b>Id</b>	1.17	-1.72	-1.51	2.68	3.20	5.53	2.85
<b>Ie</b>	1.13	-1.68	-1.54	2.67	3.21	5.49	2.82

<sup>a</sup> V<sub>S</sub> Ag/AgCl in CH<sub>3</sub>CN<sub>(l)</sub>.<sup>b</sup> V<sub>S</sub> Ag/AgCl in DMF<sub>(l)</sub>.<sup>c</sup>  $E_g^{EC}$  (Electrochemical band gap): Difference between  $E_{LUMO}$  and  $E_{HOMO}$ .<sup>d</sup>  $E_g^{Opt}$  (Optical band gap): Calculated from polymer films ( $E_g = 1240/\lambda_{onset}$ ).<sup>e</sup> The HOMO energy levels were calculated from cyclic voltammetry and were referenced to ferrocene (4.8 eV).<sup>f</sup>  $E_{1/2}$  (Average potential of the redox couple peaks).

## REFERENCES AND NOTES

- (a) Greenham, N. C.; Moratti, S. C.; Bradley, D. D. C.; Friend, R. H.; Holmes, A. B. *Nature* 1993, 365, 628–630; (b) Rothberg, L. J.; Lovinger, A. J. *J Mater Res* 1996, 11, 3174–3187; (c) Dodabalapur, A. *Solid State Commun* 1997, 102, 259–267.
- Hu, B.; Karasz, F. E. *Chem Phys* 1998, 227, 263–270.
- (a) Friend, R. H.; Gymer, R. W.; Holmes, A. B.; Burroughes, J. H.; Marks, R. N.; Taliani, C.; Bradley, D. D. C.; Dos Santos, D. A.; Bredas, J. L.; Logdlund, M.; Salaneck, W. R. *Nature* 1999, 397, 121–128; (b) Mitschke, U.; Bauerle, P. *J Mater Chem* 2000, 10, 1471–1507; (c) Hung, L. S.; Chen, C. H. *Mater Sci Eng* 2002, 39, 143–222. (d) Aziz, H.; Popovic, Z. D. *Chem Mater* 2004, 16, 4522–4532; (e) Dini, D. *Chem Mater* 2005, 17, 1933–1945.
- Gu, J.; Kawabe, M.; Masuda, K.; Namba, S. *J Appl Phys* 1977, 48, 2493–2494.
- (a) Horhold, von H. H.; Opferrmann, J. *Makromol Chem* 1970, 131, 105–132; (b) Berlan, I. B. *Handbook of Fluorescence Spectra of Aromatic Molecules*, 2nd ed.; Academic Press: New York, 1971; (c) Benzman, R.; Faulkner, L. R. *J Am Chem Soc* 1972, 94, 6317; (d) Adachi, C.; Takito, S.; Tutsui, T.; Satto, S. *Jpn J Appl Phys* 1988, 27, L269–L271; (e) Garay, R. O.; Naarmann, H.; Mullen, K. *Macromolecules* 1994, 27, 1922–1927; (f) Kim, Y. H.; Kwon, S. K.; Yoo, D. S.; Rubner, M. F.; Wrighton, M. S. *Chem Mater* 1997, 9, 2699–2701; (g) Shi, J.; Tang, C. W. *Appl Phys Lett* 2002, 80, 3201–3203; (h) Shih, H. T.; Lin, C. H.; Shih, H. H.; Cheng, C. H. *Adv Mater* 2002, 14, 1409–1412; (i) Danel, K.; Hwang, T. H.; Lin, J. T.; Tao, Y. T.; Chen, C. H. *Chem Mater* 2002, 14, 3860–3865; (j) Liu, T. H.; Shen, W. J.; Balaganesan, B.; Yen, C. K.; Iou, C. Y.; Chen, H. H.; Chen, C. H. *Synth Met* 2003, 137, 1033–1034.
- (a) Zheng, S.; Shi, J.; *Chem Mater* 2001, 13, 4405–4407; (b) Shi, J.; Tang, C. W. *Appl Phys Lett* 2002, 80, 3201–3203. (c) Li, Y.; Fung, M. K.; Xie, Z.; Lee, S. T.; Hung, L. S.; Shi, J. *Adv Mater* 2002, 14, 1317–1321; (d) Zhang, X. H.; Liu, M. W.; Wong, O. Y.; Lee, C. S.; Kwong, H. L.; Lee, S. T.; Wu, S. K. *Chem Phys Lett* 2003, 369, 478–482; (e) Kan, Y.; Wang, L.; Gao, Y.; Duan, L.; Wu, G.; Qiu, Y. *Synth Met* 2004, 141, 245–249; (f) Tao, S.; Hong, Z.; Peng, Z.; Ju, W.; Zhang, X.; Wang, P.; Wu, S.; Lee, S. *Chem Phys Lett* 2004, 397, 1–4; (g) Kan, Y.; Wang, L.; Duan, L.; Hu, Y.; Wu, G.; Qiu, Y. *Appl Phys Lett* 2004, 84, 1513–1515; (h) Lee, M. T.; Chen, H. H.; Liao, C. H.; Tsai, C. H.; Chen, C. H. *Appl Phys Lett* 2004, 85, 3301–3303; (i) Liu, T. H.; Wu, Y. S.; Lee, M. T.; Chen, H. H.; Liao, C. H.; Chen, C. H. *Appl Phys Lett* 2004, 85, 4304–4306; (j) Cao, W.; Zhang, X.; Bard, A. J. *J Electroanal Chem* 2004, 566, 409–413.
- (a) Inoue, T.; Nakaya, K. U.S. Patent 5,635,308, 1997; (b) Sui, J.; Tang, C. W. *Appl Phys Lett* 2002, 80, 3201–3203. (c) Benmansour, H.; Shioya, T.; Sato, Y.; Bazan, G. C. *Adv Funct Mater* 2003, 13, 883–886; (d) Suzuki, K.; Seno, A.; Tanabe, H.; Ueno, K. *Synth Met* 2004, 143, 89–96; (e) Kan, Y.; Wang, L.; Gao, Y.; Duan, L.; Wu, G.; Qiu, Y. *Synth Met* 2004, 141, 245–249. (f) Liu, T. H.; Wu, Y. S.; Lee, M. T.; Chen, H. H.; Liao, C. H.; Chen, C. H. *Appl Phys Lett* 2004, 85, 4304–4306. (g) Lee, M. T.; Chen, H. H.; Liao, C. H.; Tsai, C. H.; Chen, C. H. *Appl Phys Lett* 2004, 85, 3301–3303.
- (a) Ueta, E.; Nakano, H.; Shirota, Y.; *Chem Lett* 1994, 12, 2397–2400; (b) Noda, T.; Imae, I.; Noma, N.; Shirota, Y. *Adv Mater* 1997, 9, 239–241; (c) Forrest, S. R.; Burrows, P. E.; Thompson, M. E. *Chem Ind (London)* 1998, 1022; (d) Chang, S. C.; Liu, J.; Bharathan, J.; Yang, Y.; Onohara, J.; Kido, J. *Adv Mater* 1999, 11, 734–737; (e) Jonda,

- C.; Mayer, A. B. R.; Thelakkat, M.; Schmidt, H. W.; Schreiber, A.; Haarer, D.; Terrell, D. *Adv Mater Opt Electron* 1999, 9, 117–128; (f) Bach, U.; De Cloedt, K.; Spreitzer, H.; Grätzel, M. *Adv Mater* 2000, 12, 1060–1063.
9. (a) Liou, G. S.; Hsiao, S. H.; Chen, W. C.; Yen, H. J. *Macromolecules* 2006, 39, 6036–6045; (b) Liou, G. S.; Hsiao, S. H.; Huang, N. K.; Yang, Y. L. *Macromolecules* 2006, 39, 5337–5346; (c) Liou, G. S.; Huang, N. K.; Yang, Y. L. *J Polym Sci Part A: Polym Chem* 2006, 44, 4095–4107; (d) Liou, G. S.; Yen, H. J. *J Polym Sci Part A: Polym Chem* 2006, 44, 6094–6102; (e) Liou, G. S.; Huang, N. K.; Yang, Y. L. *J Polym Sci Part A: Polym Chem* 2007, 45, 48–58; (f) Liou, G. S.; Lin, S. M.; Yen, H. J. *Eur Polym Mater* 2008, 44, 2608–2618.
10. (a) Salbeck, J.; Yu, N.; Bauer, J.; Weissörtel, F.; Bestgen, H. *Synth Met* 1997, 91, 209–215; (b) Steuber, F.; Staudigel, J.; Stössel, M.; Simmer, J.; Winnacker, A.; Spreitzer, H.; Weissörtel, F.; Salbeck, J. *Adv Mater* 2000, 12, 130–133; (c) Bach, U.; Cloedt, K. D.; Spreitzer, H.; Grätzel, M. *Adv Mater* 2000, 12, 1060–1063. (d) Tokito, S.; Noda, K.; Fujikawa, H.; Taga, Y.; Kimura, M.; Shimada, K.; Sawaki, Y. *Appl Phys Lett* 2000, 77, 160–163; (e) Mikroyannidis, J. A.; Fenenko, L.; Yahiro, M.; Adachi, C. *J Polym Sci Part A: Polym Chem* 2007, 45, 4661–4670; (f) Lee, S. K.; Ahn, T.; Cho, N. S.; Lee, J. I.; Jung, Y. K.; Lee, J.; Shim, H. K. *J Polym Sci Part A: Polym Chem* 2007, 45, 1199–1209.
11. (a) Tang, C. W.; VanSlyke, S. A.; Chen, C. H. J. *Appl Phys* 1989, 85, 3610–3616; (b) Adachi, C.; Nagai, K.; Tamoto, N. *Appl Phys Lett* 1995, 66, 2679–2681; (c) Shirota, Y. *J Mater Chem* 2000, 10, 1. (d) Shirota, Y. *J Mater Chem* 2005, 15, 75–93; (e) Hsiao, S. H.; Chang, Y. M.; Chen, H. W.; Liou, G. S. *J Polym Sci Part A: Polym Chem* 2006, 44, 4579–4592; (f) Kulasi, A.; Yi, H.; Iraqi, A. *J Polym Sci Part A: Polym Chem* 2007, 45, 5957–5967; (g) Liou, G. S.; Lin, H. Y.; Hsieh, Y. L.; Yang, Y. L. *J Polym Sci Part A: Polym Chem* 2007, 45, 4921–4932; (h) Huo, L.; He, C.; Han, M.; Zhou, E.; Li, Y. *J Polym Sci Part A: Polym Chem* 2007, 45, 3861–3871; (i) Liou, G. S.; Chang, C. W.; Huang, H. M.; Hsiao, S. H. *J Polym Sci Part A: Polym Chem* 2007, 45, 2004–2014; (j) Liou, G. S.; Chang, C. W. *Macromolecules* 2008, 41, 1667–1674; (k) Hsiao, S. H.; Liou, G. S.; Kung, Y. C.; Yen, H. J. *Macromolecules* 2008, 41, 2800–2808.
12. (a) Bellmann, E.; Shaheen, S. E.; Thayumannvan, S.; Barlow, S.; Grubbs, R. H.; Marder, S. R.; Kippelen, B.; Peyghambarian, N. *Chem Mater* 1998, 10, 1668–1676; (b) Bellmann, E.; Shaheen, S. E.; Grubbs, R. H.; Marder, S. R.; Kippelen, B.; Peyghambarian, N. *Chem Mater* 1999, 11, 399–407; (c) Xiao, H. B.; Leng, B.; Tian, H. *Polymer* 2005, 46, 5707–5713; (d) Cho, J. S.; Kimoto, A.; Higuchi, M.; Yamamoto, K. *Macromol Chem Phys* 2005, 206, 635–641; (e) Sun, M. H.; Li, J.; Li, B. S.; Fu, Y. Q.; Bo, Z. S. *Macromolecules* 2005, 38, 2651–2658.
13. (a) Yang, H. H. *Aromatic High-Strength Fibers*; Wiley: New York, 1989; (b) Imai, Y. *High Perform Polym* 1995, 7, 337–345.
14. (a) Harris, F. W.; Hsu, S. L. C. *High Perform Polym* 1989, 1, 3–16; (b) Imai, Y. *React Funct Polym* 1996, 30, 3–15; (c) Hsiao, S. H.; Li, C. T. *Macromolecules* 1998, 31, 7213–7217; (d) Liou, G. S. *J Polym Sci Part A: Polym Chem* 1998, 36, 1937–1943; (e) Eastmond, G. C.; Paprotny, J.; Irwin, R. S. *Polymer* 1999, 40, 469–486; (f) Myung, B. Y.; Ahn, C. J.; Yoon, T. H. *Polymer* 2004, 45, 3185–3193; (g) Liou, G. S.; Fang, Y. K.; Yen, H. J. *J Polym Res* 2007, 14, 147–155; (h) Li, W. M.; Li, S. H.; Zhang, Q. Y.; Zhang, S. B. *Macromolecules* 2007, 40, 8205–8211.
15. Liou, G. S.; Chen, H. W.; Yen, H. J. *J Polym Sci Part A: Polym Chem* 2006, 44, 4108–4121.
16. Oishi, Y.; Mori, K.; Hirahara, H.; Fujimura, Y.; Miya, K. *Japan Patent* 11-255,723, 1999.
17. Yang, C. P.; Hsiao, S. H.; Tsai, C. Y.; Liou, G. S. *J Polym Sci Part A: Polym Chem* 2004, 42, 2416–2431.
18. Braun, C. E.; Cook, Cl. D.; Merritt, C., Jr. *Rousseau, J. E. Org Synth Collect* 1960, 4, 711–713.
19. Meisenheimer, J. *Chem Ber* 1900, 33, 3547–3549.
20. Demas, J. N.; Crosby, G. A. *J Phys Chem* 1971, 75, 991–1024.
21. (a) Yamazaki, N.; Higashi, F.; Kawabata, J. *J Polym Sci Polym Chem Ed* 1974, 12, 2149–2154. (b) Yamazaki, N.; Matsumoto, M.; Higashi, F. *J Polym Sci Polym Chem Ed* 1975, 13, 1373–1380.
22. Xue, C.; Chen, Z.; Wen, Y.; Luo, F. T.; Chen, J.; Liu, H. *Langmuir* 2005, 21, 7860–7865.
23. Liou, G. S.; Huang, H. M.; Hsiao, S. H.; Chang, C. W.; Yen, H. J. *J Polym Res* 2007, 14, 191–199.
24. Christian, R. *Chem Rev* 1994, 94, 2319–2323.
25. Cheng, E.; Sun, T. C.; Su, Y. O. *J Chin Chem Soc* 1993, 40, 551–555.